

**FABRICATION OF FREQUENCY SELECTIVE STRUCTURE AND
EVALUATION OF MICROWAVE TRANSMISSION ON ENERGY
SAVING GLASS**

LIM HUEY SIA

A thesis submitted in
fulfilment of the requirements for the award of the
Degree of Master of Electrical Engineering with Honors



Faculty of Electrical and Electronic Engineering
Universiti Tun Hussein Onn Malaysia

FEB 2015

ABSTRACT

The use of energy saving glass has become very popular in the modern day building design. This energy saving property is achieved by applying a very thin tin oxide (SnO_2) coating on one side of the glass. This coating can provide good thermal insulation to the buildings by blocking infrared rays while being transparent to visible part of the spectrum. Drawbacks of these energy saving windows is that it also attenuates the transmission of useful microwave signals through them. These signals fall within the frequency band of 0.8GHz to 2.2GHz. In order to pass these signals through the coated glass, the use of aperture type frequency selective surface (FSS) has being proposed. In the present work, SnO_2 thin film with FSS structure was fabricated using RF magnetron sputtering technique and printed circuit board technology. Deposition time, dissipation power and oxygen flow rate were varied during the sputtering deposition process. Atomic force microscopy (AFM) and field emission-scanning electron microscopy (FE-SEM) were used to analyze the surface morphology and roughness of the SnO_2 thin film. Two point electrical probe analysis was used to determine the sheet resistance and resistivity of the SnO_2 thin film. Thickness of SnO_2 thin film was measured using surface profiler. Good correlation between the surface properties and electrical properties of SnO_2 thin film was obtained. Microwave transmission through SnO_2 coated glass with FSS structure was also analyzed using network analyzer. The result of computer simulation was confirmed and consistent with the network analyzer results that showed the improvement of SnO_2 coated glass with the FSS structure. Thermal analysis demonstrated that FSS structure had allows the transmission of GSM mobile signal penetrate in the buildings while blocking the infrared light with the SnO_2 film properties.

ABSTRAK

Penggunaan kaca yang boleh menjimatkan tenaga adalah sangat popular dalam bangunan moden masa kini. Konsep kaca penjimatan tenaga boleh dihasilkan dengan menggunakan timah oksida (SnO_2) yang sangat nipis dan disalut pada satu permukaan kaca. Lapisan ini akan menebat haba dengan baik pada bangunan-bangunan, iaitu dengan menghalang sinaran inframerah daripada telus ke dalam bangunan. Salah satu kelemahan salutan SnO_2 ini adalah ia akan melemahkan penghantaran isyarat yang berguna seperti gelombang telefon daripada melalui salutan SnO_2 . Penggunaan struktur frekuensi terpilih (FSS) adalah dicadangkan untuk mengatasi masalah ini. Di dalam projek ini, lapisan SnO_2 dan struktur FSS dibentuk dengan menggunakan RF *magnetron sputtering* dan teknologi papan litar tercetak. Mikroskop tekanan atom (AFM) dan mikroskop imbasan elektron – pancaran medan (FE-SEM) telah digunakan untuk menganalisis morfologi permukaan dan kekasaran filem nipis SnO_2 . *Two point probe* digunakan untuk menentukan rintangan filem nipis SnO_2 . Ketebalan filem nipis diukur menggunakan *surface profiler*. Perkaitan yang baik di antara sifat-sifat permukaan dan sifat elektrik SnO_2 filem nipis telah ditemui. Ketebalan filem ini juga sangat berhubung kait dengan sifat-sifat elektrik filem. Kadar penembusan gelombang mikro melalui salutan SnO_2 berserta struktur FSS dikaji menggunakan *network analyzer*. Hasil simulasi komputer telah disahkan dan konsisten dengan hasil kajian *network analyzer* yang menunjukkan peningkatan dalam penembusan gelombang melalui kaca bersalut SnO_2 dengan struktur FSS. Hasil kajian suhu juga mendapati struktur FSS telah meningkatkan penghantaran isyarat GSM dengan menembusi dalam bangunan manakala menyekat pemanasan inframerah.

CONTENTS

| | | |
|------------------|--|-------------|
| | TITLE | i |
| | DECLARATION | ii |
| | DEDICATION | iii |
| | ACKNOWLEDGEMENT | iv |
| | ABSTRACT | vi |
| | CONTENTS | viii |
| | LIST OF FIGURES | xii |
| | LIST OF SYMBOLS AND ABBREVIATIONS | xix |
| CHAPTER 1 | INTRODUCTION | 1 |
| | 1.1 Background of Research | 1 |
| | 1.2 Problem Statement and Objective | 3 |
| | 1.3 Scope of Research | 3 |
| | 1.4 Outline of Thesis | 4 |
| CHAPTER 2 | LITERATURE REVIEW | 5 |
| | 2.1 Energy Saving Glass | 6 |
| | 2.2 Thin Film Deposition | 9 |
| CHAPTER 3 | RESEARCH METHODOLOGY | 11 |
| | 3.1 Radio Frequency (RF) Magnetron Sputtering Deposition | 12 |
| | 3.2 Computer Simulation Technology (CST) | 15 |
| | 3.2.1 Electromagnetic Simulation Workflow | 16 |
| | 3.3 Printed Circuit Board Technology and Fabrication of FSS Structure | 17 |
| | 3.4 Thin Film Characterization | 19 |
| | 3.4.1 Surface Profiler and Two Point Probe | |

| | | |
|--|--|-----------|
| 3.4.2 | Field Emission Scanning Electron Microscope (FESEM) and Atomic Force Microscope (AFM) | 21 |
| 3.4.3 | X-Ray Diffraction (XRD) and UV-Vis | 23 |
| 3.5 | Spectrum Analyzer, Network Analyzer, Glass and Thermal Properties | 25 |
| 3.6 | Glass Dielectric Constant Measurement | 30 |
| CHAPTER 4 ELECTROMAGNETIC SIMULATION USING CST: FSS STRUCTURE | | 31 |
| 4.1 | CST Simulation Using Various SnO ₂ Sheet Resistance Values | 32 |
| 4.1.1 | CST Simulation Using Conventional Sheet Resistance | 34 |
| 4.1.2 | CST Simulation Using Sheet Resistance of SnO ₂ Thin Film Deposited Using RF Magnetron Sputtering System | 36 |
| 4.2 | CST Simulation Using Various Shape of FSS Structure | 38 |
| CHAPTER 5 SnO₂ THIN FILM ANALYSIS | | 45 |
| 5.1 | Electrical Properties of SnO ₂ Thin Film Deposited at Various Parameters | 45 |
| 5.1.1 | Thickness and Sheet Resistance of SnO ₂ Deposited at Different Deposition Time | 46 |
| 5.1.2 | Correlation between Thickness and Sheet Resistance of SnO ₂ Thin Film | 48 |
| 5.2 | Physical properties of SnO ₂ Thin Film | 48 |
| 5.2.1 | Roughness analysis using AFM | 49 |
| 5.2.2 | FESEM Result of SnO ₂ Thin Film | 50 |
| 5.3 | Structural Composition and Optical Properties of SnO ₂ Thin Film | 51 |
| 5.3.1 | XRD Result of SnO ₂ Thin Film | 51 |
| 5.3.2 | Optical Transmission through SnO ₂ Thin | 52 |

| | | |
|------------------|--|-----------|
| | Film | |
| 5.4 | Thickness and Sheet Resistance of SnO ₂ Deposited at Different Oxygen Flow Rate | 53 |
| 5.5 | Physical properties of AFM Result for SnO ₂ thin film | 55 |
| 5.5.1 | FESEM Result of SnO ₂ Thin Film | 56 |
| 5.5.2 | XRD Result of SnO ₂ Thin Film Deposited at Different Oxygen Flow Rate | 57 |
| 5.6 | Thickness and Sheet Resistance of SnO ₂ Deposited at Different Dissipation Power | 59 |
| 5.6.1 | AFM Result of SnO ₂ Thin Film Deposited at Different Dissipation Power | 61 |
| 5.6.2 | FESEM Result of SnO ₂ Thin Film Deposited at Different Dissipation Power | 62 |
| 5.7 | XRD Result of SnO ₂ Thin Film Deposited at Different Dissipation Power | 64 |
| CHAPTER 6 | MOBILE RADIO SIGNAL TRANSMISSION AND THERMAL PROPERTIES THROUGH SnO₂ THIN FILM DEPOSITED AT VARIOUS PARAMETERS | 66 |
| 6.1 | Signal Magnitude Analysis | 67 |
| 6.1.1 | Signal Magnitude Analysis Result of SnO ₂ Film Deposited at Different Deposition Time | 68 |
| 6.1.2 | Signal Magnitude Analysis Result of SnO ₂ Film Deposited at Different Oxygen Flow Rate | 72 |
| 6.1.3 | Signal Magnitude Analysis Result of SnO ₂ Film Deposited at Different Dissipation Power | 77 |
| 6.2 | Signal Transmission Analysis | 82 |
| 6.2.1 | Signal Transmission Result of SnO ₂ Film Deposited At Different Deposition Time | 82 |



| | | |
|------------------|---|------------|
| 6.2.2 | Signal Transmission Result of SnO ₂ Film Deposited At Different Oxygen Flow Rate | 84 |
| 6.2.3 | Signal Transmission Result of SnO ₂ Film Deposited At Different Dissipation Power | 85 |
| 6.3 | Thermal Insulation Properties | 87 |
| CHAPTER 7 | CONCLUSION | 88 |
| 7.1 | Strength of this Project | 90 |
| 7.2 | Future Work | 90 |
| | REFERENCES | 92 |
| | APPENDICES | 102 |



PTTA UTHM
PERPUSTAKAAN TUNKU TUN AMINAH

LIST OF FIGURES

| | | |
|------|--|----|
| 2.1 | Illustration of energy saving glass with the FSS structure. | 8 |
| 3.1 | Flow chart to fabricate energy saving glass | 11 |
| 3.2 | Tin oxide (SnO ₂) target material. | 12 |
| 3.3 | Fluorine Tin Oxide (FTO) target material. | 12 |
| 3.4 | Schematic diagram of magnetron source. | 13 |
| 3.5 | Magnetron sputtering operation system. | 14 |
| 3.6 | Overview of RF magnetron sputtering setup. | 15 |
| 3.7 | CST studio suite 2013 used for simulation. | 15 |
| 3.8 | Basics procedure in CST simulation. | 16 |
| 3.9 | Process flow of FSS formation. | 17 |
| 3.10 | Procedure on frequency selective structure (FSS) printed on the glass. | 18 |
| 3.11 | Front illustration for the glass before and after coating. | 19 |
| 3.12 | Surface profiler Alpha Step IQ. | 20 |
| 3.13 | Electrical properties measured using 2 point probing. | 21 |
| 3.14 | Image of the FESEM (JEOL JSM-7600F) operation system. | 21 |
| 3.15 | Configuration of the FESEM (JEOL JSM-7600F) operation system. | 22 |
| 3.16 | Image of the Park System AFM (model XE-100) operation system. | 22 |
| 3.17 | Configuration of the Park System AFM (model | 23 |

| | | |
|------|---|----|
| | XE-100) and its operation. | |
| 3.18 | Glazing incidence diffraction experimental setup. | 24 |
| 3.19 | Picture of the Panalytical X'Pert Pro-MRD used for the measurement. | 25 |
| 3.20 | Illustration of UV-Vis spectrometry. | 25 |
| 3.21 | Measurement setup for spectrum analyzer. | 25 |
| 3.22 | Spectrum analyzer of Advantest R3132 used in measurement. | 26 |
| 3.23 | Experimental setup for spectrum analysis. | 26 |
| 3.24 | Measurement setup for network analyzer testing. | 27 |
| 3.25 | Picture of Rohde&Schwarz network analyzer (ZVB 4) used in the measurement. | 27 |
| 3.26 | Experimental setup for the network analyzer testing. | 28 |
| 3.27 | Measurement setup for temperature measurement. | 28 |
| 3.28 | Experimental setup for temperature measurement. | 29 |
| 3.29 | IR thermometer used in temperature measurement. | 29 |
| 3.30 | Agilent 4291B used for dielectric constant measurement. | 30 |
| 3.31 | Glass attached to the rod for measurement. | 30 |
| 4.1 | Dielectric constant measured by Agilent 4291B. | 31 |
| 4.2 | Illustration of sheet resistance measured by the 2 point probe. | 32 |
| 4.3 | Microwave transmission at various ohmic sheet resistances and without FSS structure. | 32 |
| 4.4 | Microwave transmission at various ohmic sheet resistances and with FSS structure. | 33 |
| 4.5 | Microwave transmission at 4 ohmic sheet resistances and with and without FSS structure. | 34 |
| 4.6 | Microwave transmission at 6 ohmic sheet resistances and with and without FSS structure. | 35 |

| | | |
|------|---|----|
| 4.7 | Microwave transmission at various deposition times with the FSS structure. | 36 |
| 4.8 | Microwave transmission at various oxygen flow rate with the FSS structure. | 37 |
| 4.9 | Microwave transmission at various dissipation powers with the FSS structure. | 37 |
| 4.10 | Design of cross-dipole frequency selective surface unit cell on energy saving glass. | 39 |
| 4.11 | Design of circle frequency surface unit cell on energy saving glass. | 39 |
| 4.12 | Design of pentagon frequency selective surface unit cell on energy saving glass. | 39 |
| 4.13 | Design of triangle frequency selective surface unit cell on energy saving glass. | 40 |
| 4.14 | Design of combine structure frequency selective surface unit cell on energy saving glass. | 40 |
| 4.15 | A plot demonstrating technique to measure full width half maximum, minimum transmission loss and peak frequency from the simulation result. | 41 |
| 4.16 | Transmission loss through different shapes of frequency selective surface. | 42 |
| 4.17 | Effect on different shapes through FWHM and peak frequency analysis. | 42 |
| 4.18 | Minimum transmission loss through different shapes of frequency selective structure. | 43 |
| 4.19 | Surface area etched with the minimum transmission loss with different shapes. | 44 |
| 5.1 | Thickness of SnO ₂ film under different deposition time. | 46 |
| 5.2 | Correlation between sheet resistance and resistivity of the SnO ₂ thin film under different deposition time. | 47 |

| | | |
|------|--|----|
| 5.3 | AFM image of SnO ₂ thin film deposited at (a) 10 minutes, (b) 20 minutes and (c) 30 minutes deposition time. | 49 |
| 5.4 | FESEM image of SnO ₂ thin film deposited at (a) 10minutes, (b) 20minutes and (c) 30minutes. | 50 |
| 5.5 | XRD image of SnO ₂ thin film that deposited at different deposition time. | 51 |
| 5.6 | Transmittance of SnO ₂ thin film that deposited at different deposition time. | 52 |
| 5.7 | Thickness and deposition rate of SnO ₂ film under different oxygen flow rate. | 53 |
| 5.8 | Correlation between sheet resistance and resistivity under different oxygen flow rate. | 54 |
| 5.9 | AFM image of SnO ₂ thin film deposited at (a) 0 sccm, (b) 4sccm, (c) 8sccm and 16sccm. | 55 |
| 5.10 | FESEM images of SnO ₂ thin film deposited at (a) 0sccm, (b) 4sccm, (c) 8sccm and (d) 16sccm of O ₂ flow rate. The RF power and total pressure were 225W and 8.25mTorr, respectively. | 56 |
| 5.11 | XRD image of SnO ₂ thin film that deposited at different oxygen flow rate. | 58 |
| 5.12 | Transmittance of the SnO ₂ thin film that deposited at different oxygen flow rate. | 58 |
| 5.13 | Correlation of thickness and deposition rate of SnO ₂ thin film with different dissipation power. | 59 |
| 5.14 | Correlation between sheet resistance and resistivity under different dissipation power. | 60 |
| 5.15 | AFM image of SnO ₂ thin film that deposited (a) 150W, (b) 200W, (c) 225W, (d) 250W and (e) 300W. | 62 |
| 5.16 | FESEM images of SnO ₂ thin film deposited at (a) 150W, (b) 200W, (c) 225W and (d) 250W and (e) | 63 |

300W of dissipation power. The deposition time and total pressure were 20minutes and 8.25mTorr, respectively.

| | | |
|------|--|----|
| 5.17 | XRD image of SnO ₂ thin film that deposited at different dissipation power. | 64 |
| 5.18 | Transmittance of SnO ₂ thin film that deposited at different dissipation power. | 65 |
| 6.1 | Mobile signal strength tested with spectrum analyzer at (a) 0°, (b) 15° (c) 30°. | 67 |
| 6.2 | Signal magnitude analysis on a SnO ₂ thin film with FSS structure that deposited at different deposition time | 68 |
| 6.3 | Signal magnitude analysis on a SnO ₂ thin film with FSS structure that deposited at different deposition time. | 69 |
| 6.4 | Signal magnitude analysis at 15 degree on a SnO ₂ thin film that deposited at different deposition time. | 70 |
| 6.5 | Signal magnitude analysis at 15 degree on a SnO ₂ thin film with FSS structure that deposited at different deposition time. | 70 |
| 6.6 | Signal magnitude analysis at 30 degree on a SnO ₂ thin film that deposited at different deposition time. | 71 |
| 6.7 | Signal magnitude analysis at 30 degree on a SnO ₂ thin film with FSS structure that deposited at different deposition time. | 72 |
| 6.8 | Signal magnitude analysis on a SnO ₂ thin film that deposited at different oxygen flow rate. | 73 |
| 6.9 | Signal magnitude analysis on a SnO ₂ thin film with FSS structure that deposited at different oxygen flow rate. | 73 |

| | | |
|------|--|----|
| 6.10 | Signal magnitude analysis at 15 degree on a SnO ₂ thin film that deposited at different oxygen flow rate. | 74 |
| 6.11 | Signal magnitude analysis at 15 degree on a SnO ₂ thin film with FSS structure that deposited at different oxygen flow rate. | 75 |
| 6.12 | Signal magnitude analysis at 30 degree on a SnO ₂ thin film that deposited at different oxygen flow rate. | 76 |
| 6.13 | Signal magnitude analysis at 30 degree on a SnO ₂ thin film with FSS structure that deposited at different oxygen flow rate. | 76 |
| 6.14 | Signal magnitude analysis on a SnO ₂ thin film that deposited at different dissipation power. | 77 |
| 6.15 | Signal magnitude analysis on a SnO ₂ thin film with the FSS structure that deposited at different dissipation power. | 78 |
| 6.16 | Signal magnitude analysis at 15 degree on a SnO ₂ thin film that deposited at different dissipation power. | 79 |
| 6.17 | Signal magnitude analysis at 15 degree on a SnO ₂ thin film with the FSS structure that deposited at different dissipation power. | 79 |
| 6.18 | Signal magnitude analysis at 30 degree on a SnO ₂ thin film that deposited at different dissipation power. | 80 |
| 6.19 | Signal magnitude analysis at 30 degree on a SnO ₂ thin film with the FSS structure that deposited at different dissipation power. | 81 |
| 6.20 | Signal transmission testing on a SnO ₂ thin film that deposited at different deposition time. | 82 |
| 6.21 | Signal transmission testing on a SnO ₂ thin film | 83 |

| | | |
|------|---|----|
| | with the FSS structure that deposited at different deposition time. | |
| 6.22 | Signal transmission testing on a SnO ₂ thin film that deposited at different oxygen flow rate. | 84 |
| 6.23 | Signal transmission testing on a SnO ₂ thin film with the FSS structure that deposited at different oxygen flow rate. | 85 |
| 6.24 | Signal transmission testing on a SnO ₂ thin film that deposited at different dissipation power. | 86 |
| 6.25 | Signal transmission testing on a SnO ₂ thin film with the FSS structure that deposited at different dissipation power. | 86 |
| 6.26 | Measured temperature for different samples of glass. | 87 |



LIST OF SYMBOLS AND ABBREVIATIONS

| | | |
|---------------------------------|---|---|
| d | - | Distance |
| Θ | - | Bragg angle |
| λ | - | Wavelength |
| l | - | Length |
| A | - | Area |
| w | - | Width |
| R | - | Resistance |
| Rho | - | Resistivity |
| Rs | - | Sheet Resistance |
| t | - | Thickness |
| SnO ₂ | - | Tin dioxides |
| FTO | - | Fluorine Tin Oxide |
| FSS | - | Frequency Selective Structure |
| AFM | - | Atomic Force Microscope |
| FE-SEM | - | Field Emission Scanning Electron Microscope |
| Na ₂ CO ₃ | - | Sodium Carbonate |
| NaOH | - | Sodium Hydroxide |
| XRD | - | X-Ray Diffraction |
| CST | - | Computer Simulation Technology |
| RF | - | Radio Frequency |
| CVD | - | Chemical Vapor Deposition |
| O ₂ | - | Oxygen |
| Ar | - | Argon |
| DC | - | Direct Current |
| RF | - | Radio Frequency |
| Cu | - | Copper |

| | | |
|------|---|-----------------------------------|
| PSPD | - | Position-Sensitive Photo Detector |
| Au | - | Gold |
| 2D | - | Two Dimensional |
| 3D | - | Three Dimensional |



CHAPTER 1

INTRODUCTION

1.1 Background of Research

Malaysia is a tropical country with hot and wet weather all along the years [1]. With the weather of 34°C in average, air conditioning is basic equipment in modern buildings to release the heats to outside [2]. Thus, electrical power consumption increases with the air conditioning usage in the buildings. In addition, heavy usage of air conditioning is not good for the mother earth due to depleting of ozone layer [2]. Recently, energy saving glass has been developed to overcome this problem [3–12]. Energy saving glass could help to reduce the temperature inside the buildings by reflecting the infrared light that penetrates through the building.

The most basic energy saving glass is a glass that applied with a very thin tin oxide (SnO_2) film on it. This SnO_2 material is a semiconducting oxide that have higher band gap that are suitable in the gas sensors [13–17] due to the higher free electrons in the oxygen vacant holes and thus increased the electrical conductivity of the thin film, solar cells [18], flat panels display [19] and photo catalysis [20]. However, the disadvantage of the energy saving glass is that it reflects the important electromagnetic wave such as GSM mobile signal, GPS and Bluetooth. In order to improve the electromagnetic signal inside the building, FSS had been added into the energy saving glass [6], [8], [21–24]. This FSS structure helps to enhance the electromagnetic wave inside the building. Different FSS structure will give different transmission at various frequencies. The optimized FSS structure will give the better transmission in the particular frequency.

FSS is a structure that allow the certain frequencies to passed through it while block other frequencies. The used of FSS in this project was to improve the microwave frequencies. In the past few years, many researchers had tried to apply different structure on the energy saving glass [6], [21–25]. Bandpass FSS that act as filter with single, double and triple glass used to improve the transmission of RF/microwave frequencies. The sheet resistance of the film plays a vital role in the improvement of the energy saving glass with the FSS structure. From Liu *et al* findings, decreased in sheet resistance will increase the shielding effect of the electromagnetics wave [26]. The material of the metal oxide had the effects towards the sheet resistance of the film. The transmission of the electromagnetic wave affects once the sheet resistance changed.

Besides that, most of the researchers were using the Pilkington energy saving glass to form the FSS structure on it with the laser technique [27]. In this thesis, fabrication of energy saving glass with FSS structure will be presented. The fundamental properties of coated SnO₂ thin film and its testing toward FSS applications will be discussed. These testing and analyses are needed for optimum usage of energy saving glass application at the modern design building.

Fluorine doped tin oxide (FTO) is the common material used for the energy saving glass that fabricated by Pilkington United Kingdom (UK) [28]. The technique used by Pilkington was chemical vapor deposition (CVD) technique. However, FTO material is not an environmental friendly material due to fluorine gas process which is a toxic gas. Thin film fabrication under CVD technique will require high temperature which needs more time in production.

Indium tin oxide (ITO) also been found in the microwave frequency application [29]. But, the ITO is an expensive material that will results in high production cost. In the present research, magnetron sputtering process will be used to fabricate SnO₂ thin film. The deposition was done in room temperature which had reduced the processing time and then lead to cost saving effect. Besides that, the energy saving glass available for four season country is double panels that argon gas was filled in the middle of it [6], [9], [12], [21], [28], [30] and currently none of the research was reported in Malaysia. This energy saving glass is specially designed for four season countries. While Malaysia is a tropical country that only needs a single panel of energy saving glass [31]. For single panel energy saving glass is relatively

cheaper than the double panel energy saving glass that filled with Argon gas. SnO₂ was used as the material for energy saving glass due to its high reflectivity towards the infrared light (IR) [32–34]. Besides that, SnO₂ thin film is also chemically stable that can stay long lasting [35–37].

1.2 Problem Statement and Objective

Nowadays, energy saving glass can keep the room cold at the summer and warm at the winter. But at the same time it attenuates the useful microwave frequencies such as GSM mobile signal. Because of this, a FSS structure needs to be added into energy saving glass to improve the transmission of the energy saving glass. Different design of FSS can have different of transmission on the glass. The transmission loss also been influenced by the sheet resistance of the film.

The objectives of this project are to:

1. To simulate the transmission of the microwave signal through energy saving glass with different structure of FSS.
2. To experimentally deposit tin oxide (SnO₂) on glass substrate using RF magnetron sputtering technique and evaluate its characteristics.
3. To evaluate the heat reduction, mobile radio signal transmission through the SnO₂ glass with FSS structure and without FSS structure fabricated by RF magnetron sputtering.

1.3 Scope of Research

In order to meet above objectives, this project is carried out according to below:

1. Computer simulation using CST software for different FSS structure in microwave frequencies.
2. Fabrication of FSS structure using printed circuit board technology.
3. Deposition of SnO₂ thin film using RF magnetron sputtering plasma.
4. Surface morphology, optical and electrical properties of SnO₂ thin film analyses.
5. Microwave transmission analysis in the frequency range of 0.8-2.2GHz through SnO₂ coated glass with FSS structures.

1.4 Outline of Thesis

This thesis is consists of 7 chapters. The first chapter describes an overview of this project. The second chapter explains the literature review of previous works and techniques used in this project. The third chapter presents the experimental setup and equipment used for analyses. The fourth chapter explains the SnO₂ thin film analysis on electrical, physical and optical properties. The fifth chapter describes the CST simulation with different FSS structures and sheet resistance obtains from the electrical properties of the SnO₂ film. The sixth chapter presents the microwave transmission analysis tested with spectrum and network analyzers. Finally, the last chapter described conclusion of the findings throughout the project and propose future work.



PTTA UTHM
PERPUSTAKAAN TUNKU TUN AMINAH

CHAPTER 2

LITERATURE REVIEW

Energy saving glass was widely applied in the buildings nowadays. This energy saving glass used to save the power consumption and the mother earth [38]. Malaysia is a tropical country which is hot and wet weather, throughout the year. Energy saving glass was applied a transparent metallic oxide layer on it. The metal oxide has the ability to reflect the electromagnetic radiation from penetrates into the buildings. But this metallic oxide layer also attenuates the useful signal such as GSM mobile radio signal. In order to improve the electromagnetic wave such as GSM mobile radio signal, a FSS was introduced. The main reason of applying FSS glass was to eliminate the electromagnetic radiation of infrared as much as possible and then the electromagnetic wave of GSM mobile radio signal can be passing through.

Energy saving glass had been widely explored by many researchers to obtain better transmission in microwave frequency range in the past few years [5], [9], [27], [39]. For example, Irfan *et al* had successfully design an energy saving glass with dual bandpass FSS by hard coating technique [23]. From his findings, the FSS structure able to attenuates 92.7% IR radiation. While Syed *et al* had reported that combination of low pass and high pass FSS glass had 30dB transmission improvement in the microwave frequency range [6]. Besides that, Mats *et al* reported that the transmission improvement of 10dB had been achieved with FSS window [12]. Then, Rafique *et al* had successfully designed a dual band circular loop FSS with the improvement in transmission of 26.4dB [24]. Last but not least, Ghaffer *et al* had reported that cross dipole FSS had transmission improvement in the microwave frequency range of 11.3dB [27].

FSS had broadly used in many other applications such as antenna, building and transportation. From the findings, Philippakis *et al* had reported that FSS structure can applied on the wallpaper for better transmission [21]. Besides that, Russo *et al* had successfully design FSS structure on the application of beam steering [40]. Then, Ragan *et al* had reported that FSS structure in millimeter wave integrated circuits application [41]. The application of FSS in millimeter astronomy had reported by Ge *et al* [42]. Lastly, Lee *et al* had reported that FSS structure can improve the WLAN application in his findings [43].

2.1 Energy Saving Glass

Energy saving glass had widely been developed in the past few years. The energy saving glass applied in the country which has four seasons is good that could maintain the temperature in winter or summer. But in Malaysia, energy saving glass can helps to reduce the high temperature inside the buildings even though Malaysia do not have four season. With the energy saving glass applied on the buildings will help to save a lot of the electricity bill for long term usage.

Energy saving glass is divided into two types, which are tinted film and thin film. Tinted film is well known in the market today that have the properties to reflect heats and infrared light in the automotive application. In the tinted film category, there are few types that consist of percentage of visible light and infrared transmission.

The thin film deposited on the glass with any material can defined as thin film that thickness of the film was ranging in nanometer. The differences of tinted film and thin film are on the visibility of the glass and features on it. One can feel with hand for tinted film but not for thin film. In this project, RF magnetron sputtering technique was chosen for the thin film deposition. RF sputtering is a technique that has high deposition rate, good reproducibility and good adhesion [44–46]. Kim *et al* had done his project with investigate electrical properties of SnO₂ film deposited by RF magnetron sputtering [44]. In his research, low resistivity and high mobility was found in SnO₂ thin film for gas sensor application. Shinzo *et al* reported that SnO₂ film prepared by DC magnetron sputtering applied on optoelectronics devices [45]. In the research, lowest resistivity was established at low

temperature in organic film substrates. Dan *et al* had deposited SnO₂ by RF magnetron sputtering for solar cells application [46]. In his project, oxygen partial pressures were investigated towards the resistivity of the SnO₂ film as the buffer layer of the solar cells. The findings obtain from this project was when increased the oxygen partial pressure, the resistivity of the film decreased.

Tin oxide thin film had been deposited by RF magnetron sputtering. SnO₂ film is a transparent conducting oxides that usually found in the gas sensor and solar cells application [14], [16], [18], [47–48]. From Selin *et al* findings, amorphous films has the water permeation resistance [49]. For the window in the buildings, the water resistance ability is very important to ensure that the SnO₂ film towards the heat insulation properties is maintained. Besides that, SnO₂ film also chemically stable, low resistivity and high optical transmittance that is suitable for energy saving glass applications [36], [50].

FSS is an aperture that only allows certain of frequency band to pass through it [51–52]. Different FSS structure will brings different effects on the transmission along the frequencies range. FSS structure can be added in wallpaper [21], [53] and antenna application other than energy saving glass application [8], [22–24], [30], [33], [40–42], [54–72]. FSS structure added will help to improve the electromagnetic wave such as GSM mobile signal, wireless network, GPS and bluetooth signal in the certain area [43]. The interest of frequency range in this thesis is the microwave frequencies which range between 0.8GHz to 2.2GHz.

The concept of FSS has a long history of development over years. Several applications of FSS can be applied on marketable things and military sectors to enable multiple frequency band operation. For an example, FSS concept had been applied in microwave oven which reflects at 2.45GHz microwave energies but allowing light to pass through it [73].

CST is a tool that used to simulate the FSS structure on the glass towards the transmission in the frequency range of 0.8GHz to 6GHz. It helps to analyze the transmission from the transmitter to receiver with different design and different sheet resistance to figure out the most suitable parameter or material to be used in the energy saving glass application. It will save time and cost with the pre simulation before the experimental deposition. But all the simulation in this tool is taking perfect situation that without any losses.

In the CST simulation, several shape of the FSS had been simulated and analyzed for better transmission of the electromagnetic wave that focus on 900MHz which is GSM mobile radio signal. The selected structure was analyzed by transmission loss, bandwidth and the center frequency of the transmission in the microwave range.

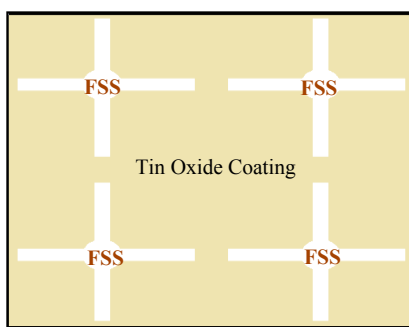


Figure 2.1: Illustration of energy saving glass with the FSS structure.

Figure 2.1 shows the energy saving glass that coated with SnO_2 film that FSS structure had been added in it. The FSS structure is specially designed to bypass the GSM mobile signals that pass through the buildings. In the energy saving glass fabrication is divided into two which are hard coating and soft coating. Hard coating means that the glass been manufactured at high temperature near 1000°C that material of energy saving glass was added in the coating process. This hard coating glass can be directly applied to buildings as window once it had been done. While for the soft coating, the coating process is separated from bare glass process. The coating was done on the surface of the bare glass. The difference between the hard coating and soft coating is the FSS structure can be formed in soft coating and not in the hard coating. Both hard and soft coating can produced energy saving glass. In this project, the aims are to investigate property of SnO_2 film with FSS in energy saving glass application. In this thesis, soft coating process was used with magnetron sputtering technique to fabricate the energy saving glass. In soft coating process, various parameters can be studied to characterize the optimum SnO_2 thin film for energy saving glass application. Hard coating means that the material is embedded in the glass when the manufacturing of the glass. While for the soft coating, it is the off-line process with the glass manufacturing. Various parameters can be changed for soft

coating process such as layer of the coating, material, deposition time to study the properties of the glass to suit the energy saving glass or other applications.

In this project, PCB technique was used to deposit FSS structure on glass. Besides that, PCB technique is widely seen in fabricating electronic devices. This PCB technique was the cheapest and fastest way in fabrication. This same technique was applied on this project with copper sheet changed to glass substrate. With that, the production cost of the energy saving glass will be cut down.

2.2 Thin Film Deposition

SnO_2 material is a tetragonal n-type semiconductor having high band gap energy ($\approx 3.6\text{eV}$) [74]. Tin oxide thin film has been reported for various applications mostly on optics, solar, transistor and gas sensor [16], [75–78]. Chemical vapor Deposition (CVD), sol-gel, electrode deposition and magnetron sputtering techniques are familiar as deposition technique used for thin film deposition. In this project, magnetron sputtering technique has been chosen due to its highly reproducible, chemically stable and high deposition rate [44], [79]. In addition, the deposition occurs at room temperature condition which is much cheaper in cost. In general, there are two sources power in magnetron sputtering technique which is Radio Frequency (RF) and Direct Current (DC). Radio frequency source is suitable for most of the target material while direct current source is more suitable for metal target material. In this project, SnO_2 was chosen as target material thus RF source power supply was chosen for magnetron sputtering deposition. Tin oxide is a fragile material, therefore the copper backing plate is required on tin oxide target. In this project, RF source power supply was chosen instead of DC source power supply was because of tin oxide is a breakable material that is not suitable for to apply DC source power supply. In RF source power supply, the power will go to auto matching box before reach the target material. While the DC source power supply, the power will directly go to target material without any auto matching box. The purpose of auto matching box was to control the power supply source constantly in the process of deposition.

From this chapter, the energy saving glass properties was studied. Soft coating method was selected because FSS structure can be formed on it. RF

magnetron sputtering technique was chosen for the SnO₂ thin film deposition. The CST simulation, FSS forming process and thin film characterization will be discussed in next chapter.



CHAPTER 3

RESEARCH METHODOLOGY

As mentioned in previous chapter, SnO₂ thin film was prepared using magnetron sputtering machine. Several analyses were carried out such as surface profiler, FESEM and AFM. The analysis is required to find the suitable parameter to fabricate an energy saving glass that can reflect most of the infrared while maintains good GSM signals. Besides that, sheet resistance of the thin film also takes into account to simulate the transmission along the GSM mobile signals. Different sheet resistance will bring effect to the transmission of microwave frequencies.

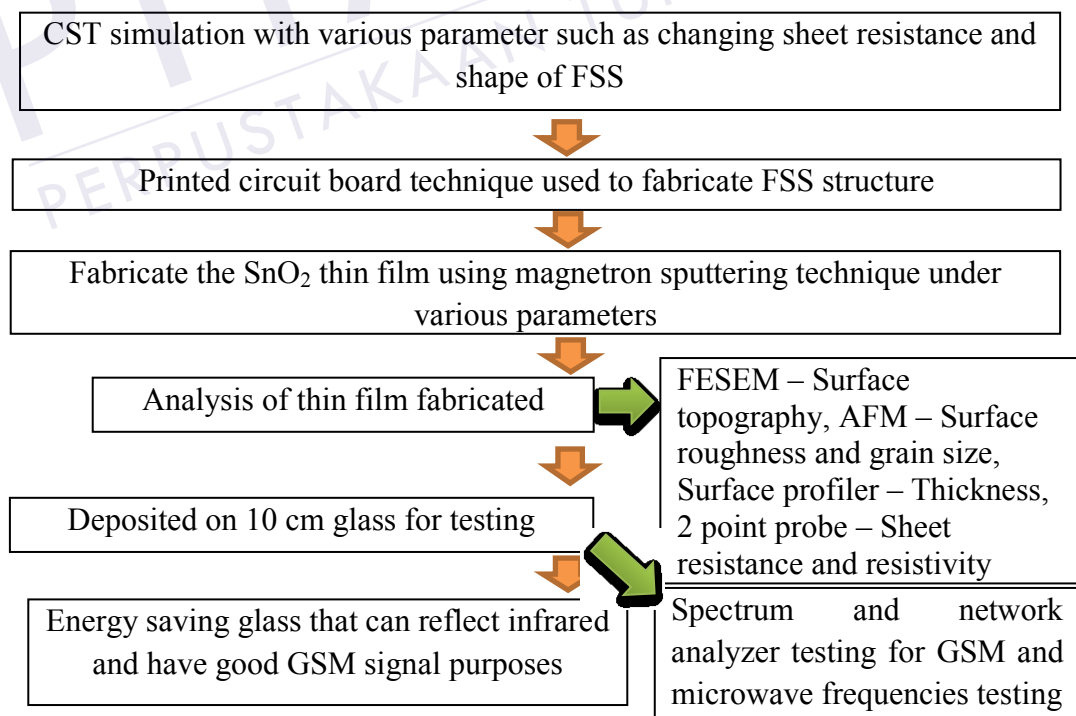


Figure 3.1: Flow chart to fabricate energy saving glass.

Figure 3.1 shows the process flow in fabricate energy saving glass. First, changing sheet resistance and shape of FSS was varied in the CST simulation. After that, FSS structure was formed by printed circuit board technique. The fabricated FSS structure on glass was deposited by magnetron sputtering to form SnO_2 thin film. Several analyses were used to analyze SnO_2 thin film such as surface topography, surface roughness and electrical properties. The deposited glass tested using spectrum and network analyzer to check the magnitude and transmission along the microwave frequencies.

3.1 Radio Frequency (RF) Magnetron Sputtering Deposition



Figure 3.2: Tin oxide (SnO_2) target material.



Figure 3.3: Fluorine Tin Oxide (FTO) target material.

Figure 3.2 shows the SnO₂ target material that used for magnetron sputtering deposition. This target had 3” diameter in size with thickness of 0.5” and the color of the target is nearly white. The copper backing is needed for the compound and fragile material. Figure 3.3 displays the FTO target that used for deposition process. The color of the FTO target was seen darker than SnO₂ target. For the FTO material, the coating on the glass will be less transparent than SnO₂ film. For the windows application in the buildings, transparency of the glass is a very important.

In sputtering process, a target is bombarded by energetic ions generated in glow discharge plasma. The bombardment process caused the removal of target atoms, which condense on a substrate as a thin film. Besides that, ion bombardment process also produced secondary electrons from the target surface. This secondary electron plays an important role in maintaining the plasma. Magnetrons are the concept of magnetic field configured parallel to the target surface can constrain secondary electron motion to the vicinity of the target. In the magnetron sputtering deposition, various parameters can be varied such as substrates bias voltage, substrate temperature, dissipation power, oxygen flow rate, deposition time and working pressure of the chamber. Vary parameters can be affects towards the film properties [46], [80–81].

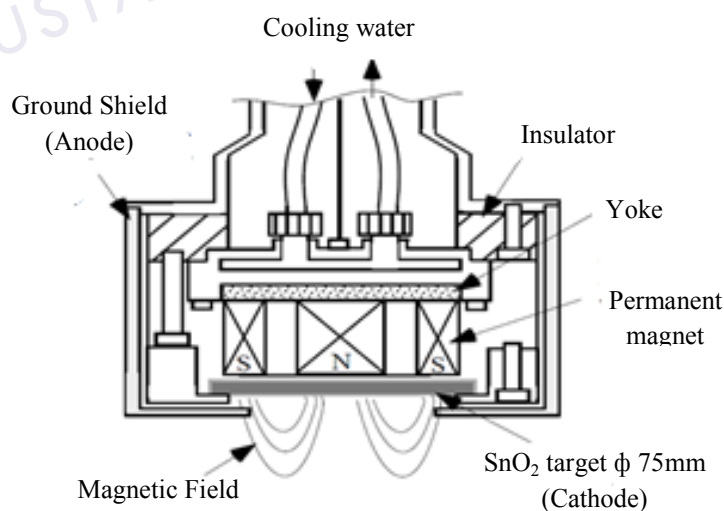


Figure 3.4: Schematic diagram of magnetron source [82].

The base pressure was kept at below 5.0×10^{-6} mTorr before the deposition started to ensure the film quality. Due to SnO_2 is a fragile material, the deposition was done in changed the dissipation power between 150W to 300W. Gas pressure used in the system was 8.25mTorr when the deposition of SnO_2 film on the glass substrate. Two gases were used in the deposition process which is argon (Ar) and oxygen (O_2) gas. The gas flow rate for Ar was 25sccm with the various oxygen flow rate was changed. The oxygen flow rate changed in between 0sccm, 4sccm, 8sccm and 16sccm. Figure 3.4 shows the schematic diagram of the magnetron sputtering system used in this project. In the system, the ground shield is representative as anode while SnO_2 target as cathode. The system was connected to the chiller that acts as cooling water into it. Permanent magnet connected to SnO_2 target creates magnetic field when dissipation power applied on it.

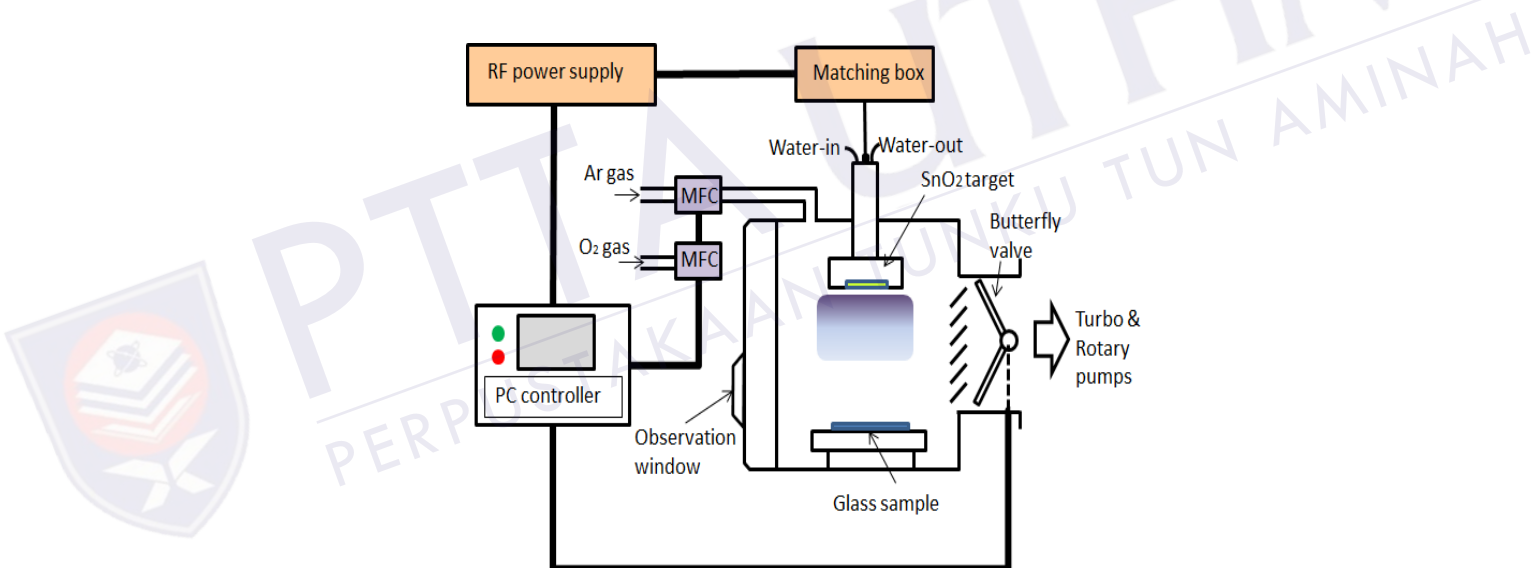


Figure 3.5: Magnetron sputtering operation system.

Figure 3.5 displays the illustration of the RF magnetron sputtering system. In the system, the target was placed 11cm from the glass substrate. The angle of the SnO_2 target was around 45° to the glass substrate. Before the deposition started, high vacuum condition is required to produce high quality SnO_2 film. In order to achieve high vacuum, rotary pump and turbo pump had been used. Deposition process happened with the Ar and O_2 gas that supply into the chamber. Other than gases,

dissipation power and gas pressure also need to be set before the deposition process start.



Figure 3.6: Overview of RF magnetron sputtering setup.

Ion bombardment influenced the films produced on the substrate by structure and electrical properties. Besides that, the energy of the bombardment ions can be increased by increasing the negative bias applied to the substrate. However, when the negative bias increased it can bring defects in the film and decreased the overall film properties [83]. Figure 3.6 shows the RF and DC sputtering system that available at MiNT-SRC UTHM.

3.2 Computer Simulation Technology (CST)

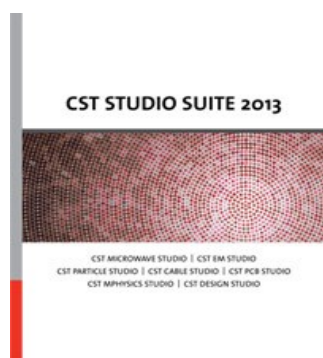


Figure 3.7: CST studio suite 2013 used for simulation.

Computer Simulation Technology (CST) simulation is 3D electromagnetic simulation software that can design and optimize the operating devices in a wide range of frequencies. Frequency domain solver was chosen over transient domain solver due to it is suitable for periodic structures application such as FSS. Besides that, CST microwave studio features a special periodic boundary implementation that creates for unit cells shaped. Floquet mode port was used in the port mode that produces higher accuracy and fast simulation to ease the polarization analysis and mode type. CST simulation was used Finite Integration Technique (FIT) that can simulate two materials together as metal oxide layer that stack above the glass that used in this project. In this project, CST simulation was used due to the mesh size required was two mesh. Figure 3.7 shows the CST studio suite 2013 used in simulation for this project. In the CST simulation, there are two solver to solve the problems, transient and frequency simulation. Transient solver is used in order to obtain accurate broadband results in the frequency domain where the electromagnetic energy in the computational domain needs to be sufficiently decayed. Basically, transient solver is use to solve electrically medium and large sized problems. It is suitable for broadband analysis.

The steady state behavior of a model simulated using frequency domain simulation is calculated at different frequency points. It is suitable to run the simulation in narrow band or single frequency. This frequency domain is normally applied on electrically small or medium sized problems. Frequency domain is simulating in periodic structures with Floquet port modes. The step by step in CST simulation part was in Appendix A.

3.2.1 Electromagnetic Simulation Workflow

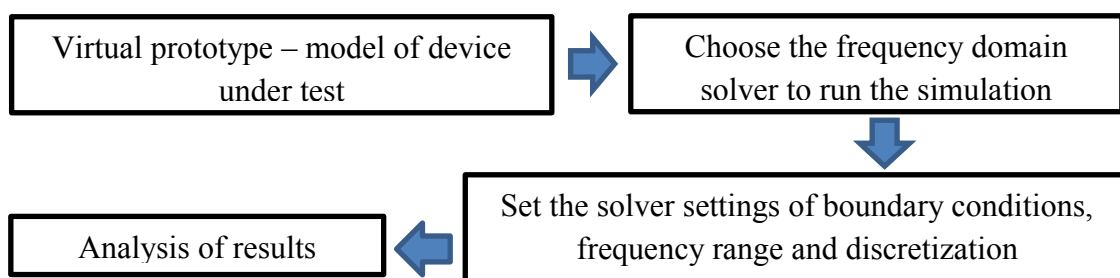


Figure 3.8: Basics procedure in CST simulation.

Figure 3.8 shows the basic procedure in running the CST simulation. In the CST simulation, the transmission of the signal between transmitter and receiver can be obtained in perfect condition without any loss.

3.3 Printed Circuit Board Technology and Fabrication of FSS Structures

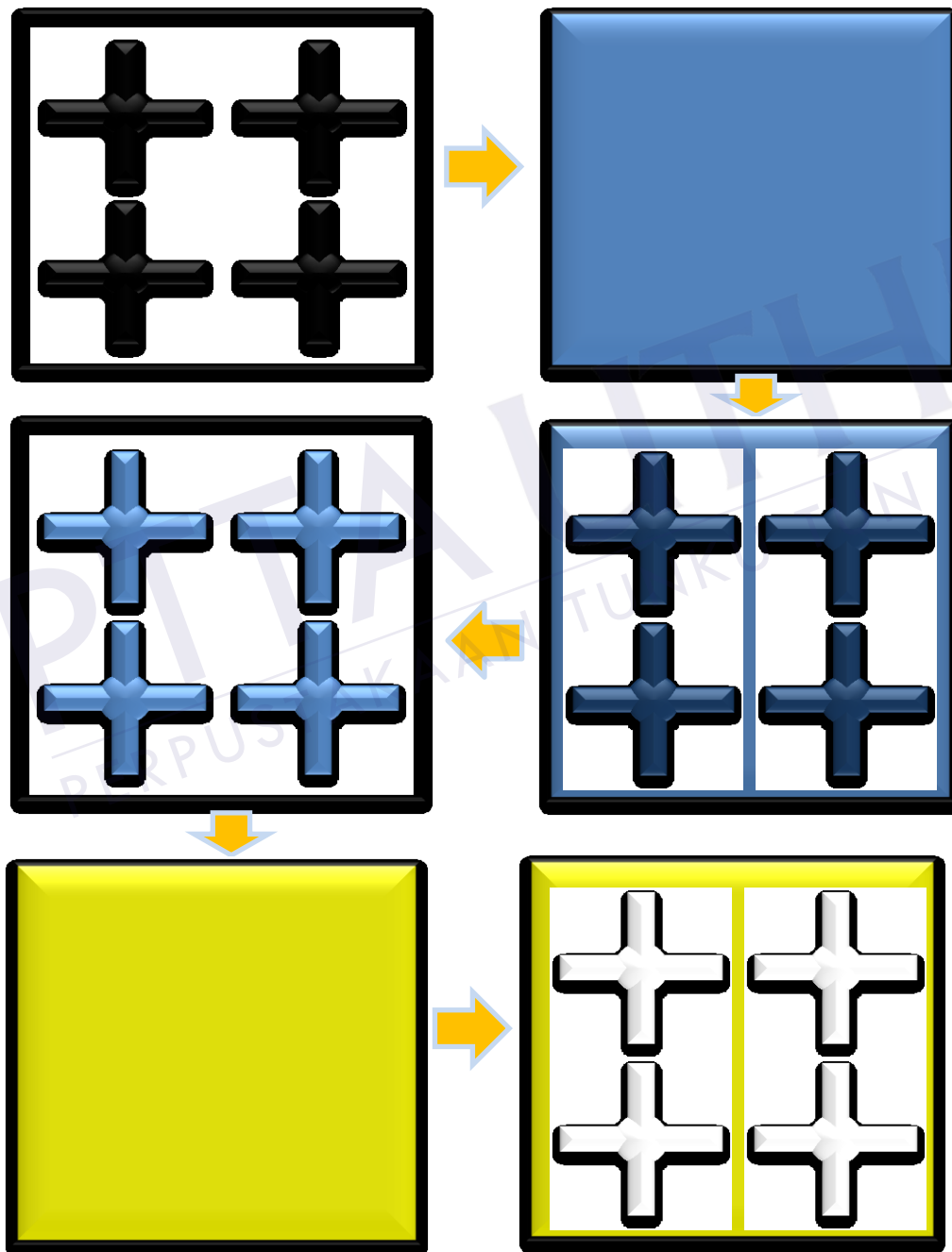


Figure 3.9: Process flow of the FSS formation.

Printed circuit board (PCB) technique was chosen in this project due to its simplicity and low cost in fabricating the FSS structure. Besides that, this technology can easily found in the electronic labs that ease for the experiment. The advantage of the PCB technique compare to the laser technique was the process of fabrication. The PCB fabrication process was easier than laser fabrication process due to the laser etching required CO₂ gas.

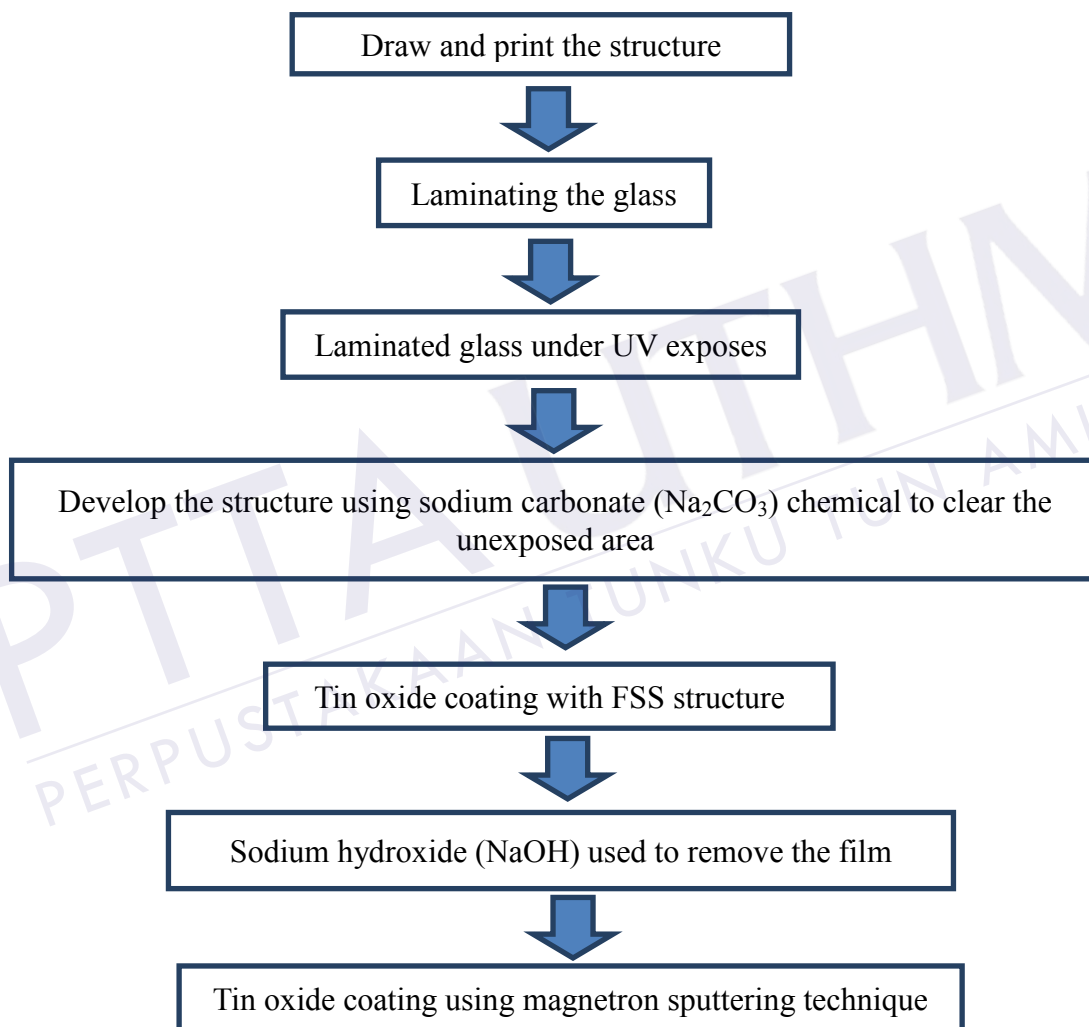


Figure 3.10: Procedure on frequency selective structure (FSS) printed on the glass.

Regarding the fabrication accuracy, there were around 80% successfully with handling every process carefully. For laminating part, bubbles were not allowed on the glass. Time control in the UV expose was one of the key points for the fabrication process. Glass with the FSS structure developed need to be under the sun heating for strengthens the attraction force. After that, fabrication process was done

in high vacuum condition to avoid contamination of film. For the etching film, the film will not be degraded as the RF deposition technique had the strong adhesion as other deposition technique. The repeatability of the PCB fabrication process was quite high around 95%. The difference process on this experiment is usually copper or aluminum board will be used in etching purposes to form the structure on it and this project is using glass to replace it. Glass is used due to the energy saving glass application in this project. Figure 3.10 shows the process flow chart of the FSS fabrication on the glass substrate and can best describe the FSS fabrication on the glass.

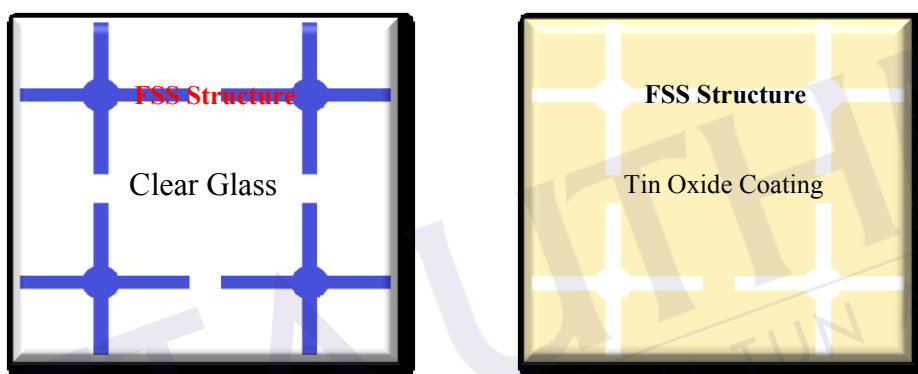


Figure 3.11: Front illustration for the glass before and after coating.

Figure 3.11 shows the glass before and after coating for the energy saving glass fabrication.

3.4 Thin Film Characterization

Several techniques have been used in the thin film analysis such as field emission scanning electron microscopy (FESEM), atomic force microscopy (AFM) and 2 point probe. Thickness of the film was analyzed by surface profiler. Electrical properties were analyzed by 2 point probe. Sheet resistance and resistivity of the SnO_2 film can be obtained from the electrical properties analysis. This sheet resistance is the key parameter that will effect to the transmission of electromagnetic wave.

FESEM analysis was to investigate the structure and grain size of the SnO_2 particle. While AFM analysis was to analyzed film roughness. The difference with

the FESEM and AFM is 2D and 3D images obtained. Transparency of the glass is very important for the window application in the buildings. UV-Vis is a tool that used for the glass transparency measurement. Physical composition of the SnO₂ film was analyzed by X-Ray Diffraction (XRD) technique. This analysis was to determine the changes state of the SnO₂ film with various parameters. All the analyses about will be relate to the result of the thermal insulation properties and the transmission of the electromagnetic wave. Details of this equipment will be discussed in research methodology.

3.4.1 Surface Profiler and Two Point Probe



Figure 3.12: Surface profiler Alpha Step IQ.

Thickness of the thin film is important in order to characterize it in energy saving glass application for this project. With the measurement of the thin film thickness, sheet resistance of the thin film can be calculated. Sheet resistance is an important key to improve the GSM transmission in the energy saving glass [27]. Picture of the surface profiler is show in Figure 3.12.

For the two point probe method, the current and voltage are measured in the same wire. In this case, the measured voltage is added with the potential difference created into wires. While for the four point probe, current is sent in two probes and voltage is measured by two other probes. So, the measured voltage is circulating into the sample without current. Meanwhile, it means that the potential difference into wires and area of contact and spreading resistances are not high. In this project, two point probing is used for the electrical properties of the thin film.

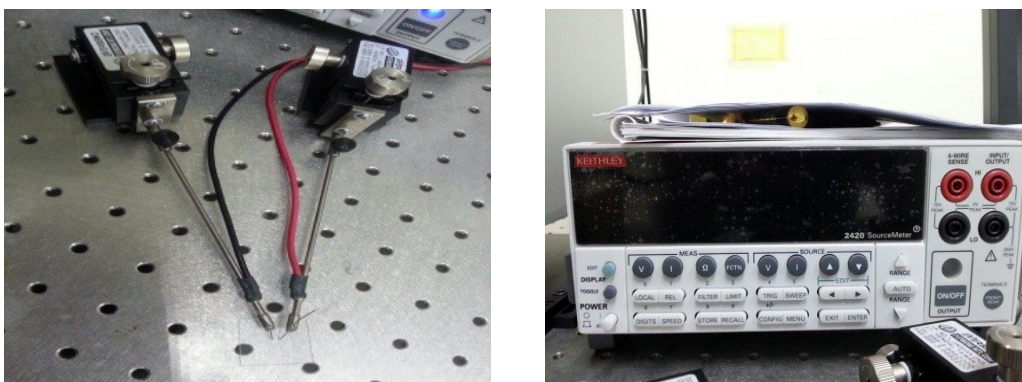


Figure 3.13: Electrical properties measured using 2 point probing.

Figure 3.13 shows the two point probing that used to measure electrical properties of the thin film. From the IV graph obtained from the two point probing, resistivity can be calculated by Equation 3.1. Sheet resistance of the film can be calculated by Equation 3.2 with the resistivity obtained from Equation 3.1. Besides than the thickness and the sheet resistance of the film, dielectric constant of the glass also take into the account when the CST simulation.

$$\text{Resistance, } R = \text{Resistivity, } \rho \times \frac{\text{Length, } l}{\text{Area, } A} = \left(\frac{\rho}{\text{Thickness, } t} \right) \times \left(\frac{l}{\text{Width, } w} \right) \quad (3.1)$$

$$\text{Sheet resistance, } R_s = \frac{\rho}{t} \quad (3.2)$$

3.4.2 Field Emission Scanning Electron Microscope (FESEM) and Atomic Force Microscope (AFM)



Figure 3.14: Image of the FESEM (JEOL JSM-7600F) operation system.

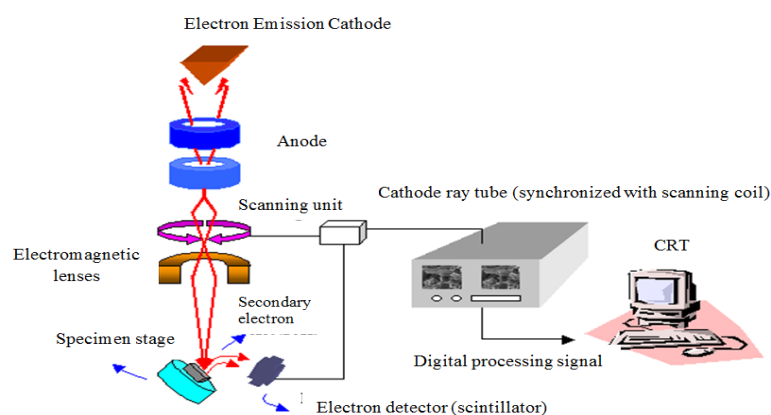


Figure 3.15: Configuration of the FESEM (JEOL JSM-7600F) operation system [84].

FESEM is a microscope that operates with electrons to form the morphology image for the surface object [84]. Dry sample is required to achieve high vacuum condition in scanning process. This system has two electrons operated which are primary and secondary electrons. Primary electrons can be achieved at high vacuum condition and then been focused and deflected to scanning unit to produce a narrow beam that will have bombardment on the object [84]. Surface structure of the thin film is affected by angle and velocity of the secondary electron. Electron detector detects the secondary electron and sent the information to scanning unit. Morphology of the thin film can be seen in computer screen after digital signal processing process the data in the scanning unit. The operation system of the FESEM analysis is clearly showed in Figure 3.14 and 3.15.



Figure 3.16: Image of the Park System AFM (model XE-100) operation system.

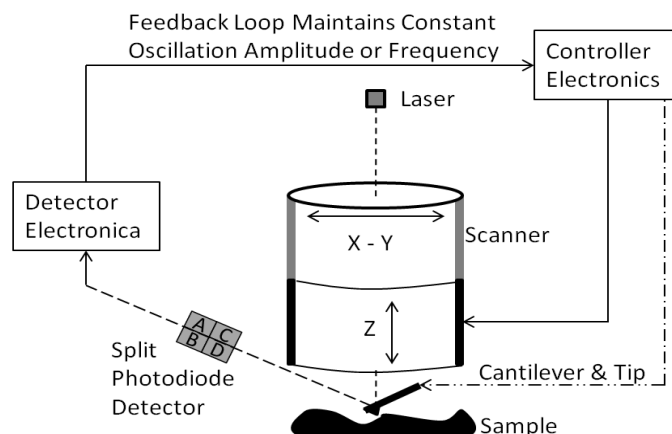


Figure 3.17: Configuration of the Park System AFM (model XE-100) and its operation [86].

The measurement of the AFM is in three dimensions, which are x and y in horizontal with z in vertical direction. In atomic force microscopy (AFM) are divided into three, which are contact, non-contact and tapping mode. For contact and tapping mode, the cantilever had touched the sample that will damage the sample.

While, non-contact AFM is a laser beam is used to deflect the cantilever passes over a sample that will go through the position sensitive photo detector (PSPD) and come out with topological surface of the sample [85]. The system used is non-contact AFM that cantilever vibrate near resonant frequency that ranging between 100 kHz and 400 kHz [85]. Roughness of the film can be obtained with the AFM measurement. The advantages of the AFM compare to FESEM were AFM has 3D image and FESEM has 2D image for the film structure. Figure 3.16 shows the picture and operation of the AFM measurement. Figure 3.17 shows the operation system for AFM.

3.4.3 X-Ray Diffraction (XRD) and UV-Vis

X-Ray Diffraction (XRD) used in this project to differentiate the chemical formula that change during changes of parameter in the deposition. XRD is a non-destructive analytical technique for identification and quantitative determination of the solid sample. Glazing incidence diffraction (GID) is used in analyzed thin film due to its

small diffracting volumes that caused low diffracted intensities [86]. When analyzing thin film, parallel beam geometry is combined with glazing incidence angle to obtain the spectrum peaks. The detector is rotates through the angular range while others is remain constant in the collecting of the spectrum diffraction [86]. The XRD analysis was best described by Bragg's Law as Equation 3.3.

$$n\lambda = 2d\sin\theta \quad (3.3)$$

Where n represents integer, λ symbolize the wavelength of the incident X-ray beam, d is the distance between the atomic layers in crystal and θ is the incident angle of the X-ray beam.

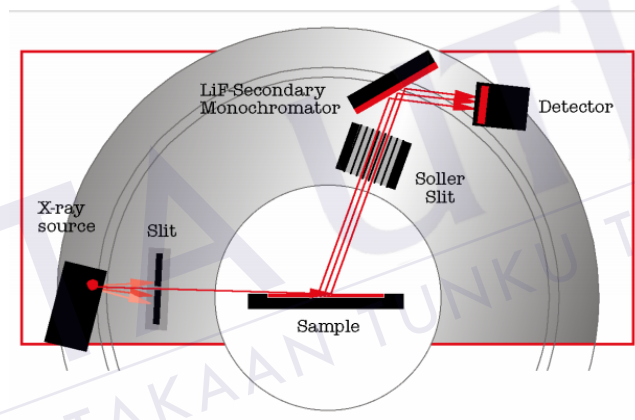


Figure 3.18: Glazing incidence diffraction experimental setup [86].



Figure 3.19: Picture of the Panalytical X'Pert Pro-MRD used for the measurement.

REFERENCES

1. 2014. A Global Review. *Irrigation & Drainage in the World*. Retrieved Dec 14, 2014, from http://www.icid.org/i_d_malaysia.pdf
2. R. Heede. (2013). Tracing anthropogenic carbon dioxide and methane emissions to fossil fuel and cement producers, 1854–2010. *Clim. Change*, 122(1-2), pp. 229–241.
3. S. H. Sohail, G. I. Kiani, and K. P. Esselle. (2011). Parametric Analysis of RF and Microwave Transmission through Single and Multiple Layer of Float Glass. *Proceeding Asia-Pacific Microw. Convergence*, 2, pp. 1454–1457.
4. A. Z. Khan. (1966). Electrical energy conservation and its application to a sheet glass industry. *IEEE Trans. energy Convers.*, 11(3), pp. 666–671.
5. G. I. Kiani, L. G. Olsson, A. Karlsson, and K. P. Esselle. (2010) Transmission of infrared and visible wavelengths through energy-saving glass due to etching of frequency-selective surfaces. *IET Microwaves, Antennas Propag.*, 4(7), pp. 955-961.
6. G. I. Kiani, A. R. Weily and K. P. Esselle. (2006). A novel absorb/transmit FSS for secure indoor wireless networks with reduced multipath fading. *IEEE Microwave Wireless Components Letter*, 16(6), pp. 378–380.
7. Q. H. Li, A. H. Meng and Y. G. Zhang. (2009). Recovery Status and Prospect of Low-grade Waste Energy in China. *Sustainable Power Generation and Supply*, pp. 1–6.

8. S. I. Sohail, K. P. Esselle and G. Kiani. (2012). Design of a Bandpass FSS on Dual Layer Energy Saving Glass for Improved RF Communication in Modern Buildings. *Antennas and Propagation Society International Symposium*, pp. 1–2.
9. I. Ullah, D. Habibi and G. Kiani. (2011). Design of RF/Microwave efficient buildings using frequency selective surface. *2011 IEEE 22nd Int. Symp. Pers. Indoor Mobile Radio Communication*, pp. 2070–2074.
10. N. Yamauchi, T. Itoh and T. Noguchi. (2012). Low energy-cost TFT technologies using ultra thin flexible glass substrate. *19th International Workshop on Active-Matrix Flatpanel Displays and Devices*, pp. 213–214.
11. C. Yang, D. Yuan, and Y. Jia. (2012). Research on energy of an office building equipped high permeability with Low-E window in Xinxiang. *2012 2nd International Conference Consumer Electronics Communication Networks*, pp. 508–511.
12. M. Gustafsson, A. Karlsson, A. P. P. Rebelo, and B. Widenberg. (2006). Design of Frequency Selective Windows for Improved Indoor Outdoor Communication. *IEEE Transaction Antennas Propagation*, 54(6), pp. 1897–1900.
13. R. R. Kasar, N. G. Deshpande, Y. G. Gudage, J. C. Vyas, and R. Sharma. (2008). Studies and correlation among the structural, optical and electrical parameters of spray-deposited tin oxide (SnO₂) thin films with different substrate temperatures. *Physics B Condensation Matter*, 403(19-20), pp. 3724–3729.
14. G. Korotcenkov and B. K. Cho. (2009). Thin film SnO₂-based gas sensors: Film thickness influence. *Sensors Actuators B Chemistry*, 42(1), pp. 321–330.
15. E. Comini, G. Faglia, and G. Sberveglieri. (2001). UV light activation of tin oxide thin Films for NO₂ sensing at low temperatures. *Sensors and Actuators B: Chemical*, 78(1-3), pp. 73–77.

16. V. V Kissine, S. A. Voroshilov, and V. V Sysoev. (1999). Oxygen flow effect on gas sensitivity properties of tin oxide film prepared by r.f. sputtering. *Sensors Actuators B: Chemical*, 55(1), pp. 55–59.
17. R. Dolbec, M. a. El Khakani, a. M. Serventi, and R. G. Saint-Jacques. (2003). Influence of the nanostructural characteristics on the gas sensing properties of pulsed laser deposited tin oxide thin films. *Sensors Actuators B: Chemical*, 93(1-3), pp. 566–571.
18. S. Lee, J. Lee, T. Oh, and Y. Kim. (2003). Fabrication of tin oxide film by sol – gel method for photovoltaic solar cell system. *Solar Energy Materials and Solar Cells*, 75(3-4), pp. 481–487.
19. D. M. Mukhamedshina and N. B. Beisenkhanov. (2006). Chapter 9: Influence of Crystallization on the Properties of SnO₂ Thin Films. *Advances in Crystallization Processes Dr. Yitzhak Mastai (Ed.)*.
20. S. Sen and V. B. Patil. (2013). Nanocrystalline SnO₂ thin films : Structural , morphological , electrical transport and optical studies. *Journal of Alloys and Compounds*, 563, pp. 300–306.
21. M. Philippakis, C. Martel, D. Kemp, S. Appleton, and R. Pearson. (2004). Application of FSS Structures to Selectively Control the Propagation of signals into and out of buildings. *Antenna Systems(Era Technology)*, pp. 1–54.
22. P. T. Teo, X. F. Luo, and C. K. Lee. (2007). Frequency-selective surfaces for GPS and DCS1800 mobile communication , Part 1 : Quad-layer and single-layer FSS design. *IET Microwaves Antennas Propagation*, 1(2), pp. 314–321.
23. I. Ullah, X. Zhao, and G. K. Habibi, Daryoush. (2011). Transmission improvement of UMTS and Wi-Fi signals through energy saving glass using FSS. *Wireless and Microwave Technology Conference*, pp. 1-5.

24. U. Rafique, M. M. Ahmed, S. Member, M. A. Haq, and M. T. Rana. (2011). Transmission of RF Signals through Energy Efficient Window Using FSS. 7th Conference On *Emerging Technologies (ICET)*, pp. 1–4.
25. G. Kiani, L. Olsson, A. Karlsson, and K. Esselle. (2008). Transmission analysis of energy saving glass windows for the purpose of providing FSS solutions at microwave frequencies. *Antennas and Propagation Society International Symposium*, pp. 25–28.
26. J. Tan, Y. Liu. (2013). Frequency dependent model of sheet resistance and effect analysis on shielding effectiveness of transparent conductive mesh coatings. *Progress Electromagnetic Research*, 140, pp. 353–368.
27. G. I. Kiani, L. G. Olsson, A. Karlsson, K. P. Esselle, S. Member, and M. Nilsson. (2011). Cross-Dipole Bandpass Frequency Selective Surface for Energy-Saving Glass Used in Buildings. *IEEE Transactions on Antennas and Propagation*, 59(2), pp. 520–525.
28. Energy Saving Glass - Warm Coatings. *Pilkington*, Retrieved May 14, 2014, from <http://www.pilkington.com/coatings.htm>
29. C. Tsokonas. (2001). Optically transparent frequency selective window for microwave applications. *Electronics Letters IET*, 37(24), pp. 20–22.
30. B. Widenberg, J. Víctor, and R. Rodríguez. (2002). Design of Energy Saving Windows with High Transmission at 900 MHz and 1800 MHz. *CODEN: LUTEDX(TEAT-7110)*, pp. 1-14.
31. N. B. Huat and Z. Abidin (2011). An Overview of Malaysia Green Technology Corporation Office Building: A Showcase Energy-Efficient Building Project in Malaysia. *J. Sustain. Dev.*, 4(5), pp. 212–228.
32. M. Batzill and U. Diebold. (2005). The surface and materials science of tin oxide. *Prog. Surf. Sci.*, 79(2-4), pp. 47–154.

33. C. Mias, C. Tsakonas, C. Oswald, and B. Street. (2011). Department of Electrical and Electronic Engineering An Investigation into the Feasibility of designing Frequency Selective Windows employing periodic structures (Ref . AY3922) Final Report for The Radiocommunications Agency. *The NottinghamTrent University,Electrical and Electronics Department, 44*, pp. 1-167.
34. M. Maleki and S. M. Rozati. (2013). An economic CVD technique for pure SnO₂ thin films deposition: Temperature effects. *Bull. Mater. Sci.*, 36(2), pp. 217–221.
35. M. Alaf, M. O. Guler, D. Gultekin, M. Uysal, A. Alp, and H. Akbulut. (2008). Effect of oxygen partial pressure on the microstructural and physical properties on nanocrystalline tin oxide films grown by plasma oxidation after thermal deposition from pure Sn targets. *Vacuum*, 83(2), pp. 292–301.
36. A. Faheem, M. Mehmood, A. M. Rana, and M. T. Bhatti. (2009). Applied Surface Science Effect of annealing on electrical resistivity of rf-magnetron sputtered nanostructured SnO₂ thin films. *Chinese Physics Letters*, 26(7), pp. 8562–8565.
37. Z. W. Chen, G. Liu, H. J. Zhang, G. J. Ding, Z. Jiao, M. H. Wu, C. H. Shek, C. M. L. Wu, and J. K. L. Lai. (2009). Insights into effects of annealing on microstructure from SnO₂ thin films prepared by pulsed delivery. *J. Non. Cryst. Solids*, 355(52-54), pp. 2647–2652.
38. B. F. Yu, Z. B. Hu, M. Liu, H. L. Yang, Q. X. Kong, and Y. H. Liu. (2009). Review of research on air-conditioning systems and indoor air quality control for human health. *Int. J. Refrig.*, 32(1), pp. 3–20.
39. C. Chen, S. Chen, W. Chuang, and J. Shieh. (2011). Transparent Glass Window with Energy-saving and Heat Insulation Capabilities. *Advances Materials Reseach*, 316, pp. 10–16.

40. I. Russo, L. Boccia, G. Amendola, G. Di Massa, and V. P. Bucci. (2010). Tunable Pass-Band FSS for Beam Steering Applications. *Proceeding of the Fourth European Conference on Antennas and Propagation*, pp. 1-4.
41. L. Ragan, A. Hassibi, T. S. Rappaport, and C. L. Christianson. (2007). Novel On-Chip Antenna Structures and Frequency Selective Surface (FSS) Approaches for Millimeter Wave Devices. *2007 IEEE 66th Veh. Technol. Conf.*, pp. 2051–2055.
42. G. Wu, V. Hansen, E. Kreysa, and H.-P. Gemuend. (2006). Design and Optimization of FSS Structures for Applications in (Sub) millimetre Astronomy Using a PSO Algorithm. *2006 Jt. 31st Int. Conf. Infrared Millim. Waves 14th Int. Conf. Teraherz Electron.*, (2), pp. 401.
43. L. Y. Seng, M. F. Abd Malek, W. F. Hoon, L. W. Leong, N. Saudin, L. Mohamed, N. A. Mohd Affendi, and A. B. Ali, “Frequency selective surface for enhance WLAN applications,” *2012 IEEE Symp. Wirel. Technol. Appl.*, vol. 2, no. 12, pp. 81–84, Sep. 2012.
44. I. H. Kim, J. H. Ko, D. Kim, K. S. Lee, T. S. Lee, J. -h. Jeong, B. Cheong, Y.-J. Baik, and W. M. Kim. (2006). Scattering mechanism of transparent conducting tin oxide films prepared by magnetron sputtering. *Thin Solid Films*, 515(4), pp. 2475–2480.
45. T. S. M. Tadatsugu, N. Hidehito. (1988). Highly Conducting and Transparent SnO₂ Thin Films Prepared by RF Magnetron Sputtering on Low-Temperature Substrates. *Japanese J. Appl. Physics*, 27(3), pp. 287–289.
46. D. Leng, L. Wu, H. Jiang, Y. Zhao, J. Zhang, W. Li, and L. Feng. (2012). Preparation and Properties of SnO₂ Film Deposited by Magnetron Sputtering. *Int. J. Photoenergy*, 2012, pp. 1–6.
47. L. P. Chikhale, J. Y. Patil, a. V. Rajgure, F. I. Shaikh, I. S. Mulla, and S. S. Suryavanshi. (2014). Structural, morphological and gas sensing properties of

- undoped and Lanthanum doped nanocrystalline SnO₂. *Ceram. Int.*, 40(1), pp. 2179–2186.
48. L. Sangaletti, L. E. Depero, A. Dieguez, G. Marca, and J. R. Morante. (1997). Microstructure and morphology of tin dioxide multilayer thin film gas sensors. *Sensors and Actuators B*, 44 , pp. 268–274.
 49. B. S. Tosun, R. K. Feist, A. Gunawan, K. A. Mkhoyan, S. a. Campbell, and E. S. Aydil. (2012). Sputter deposition of semicrystalline tin dioxide films. *Thin Solid Films*, 520(7), pp. 2554–2561.
 50. B. Thangaraju, “Structural and electrical studies on highly conducting spray deposited fluorine and antimony doped SnO₂ thin films from SnCl₂ precursor. (2002). *Thin Solid Films*, 402(1-2), pp. 71–78.
 51. M. Z. A. A. Aziz, M. M. Shukor, M. K. Suaidi, B. H. Ahmad, M. F. Johar, S. N. Salleh, F. A. Azmin, and M. F. A. Malek. (2013). Impedance of the unit cell of the frequency selective surface at 2.4 GHz. *2013 3rd Int. Conf. Instrumentation, Commun. Inf. Technol. Biomed. Eng.*, 5(5), pp. 49–53.
 52. M. Z. A. A. Aziz, M. M. Shukor, B. H. Ahmad, M. K. Suaidi, M. F. Johar, M. A. Othman, S. N. Salleh, F. a. Azmin, and M. F. A. Malek. (2013). Investigation of a square loop Frequency Selective Surface (FSS) on hybrid material at 2.4 GHz. *2013 IEEE Int. Conf. Control Syst. Comput. Eng.*, pp. 275–278.
 53. 2006. Periodic Arrays: FSS and PBG. *CST Studio Suite 2006B Application Note*. Retrieved Dec 14, 2014, from <http://www.cst.com>.
 54. R. A. Pearson, B. Phillips, K. G. Mitchell, and M. Patel. (1996). Application of Waveguide Simulators to FSS and Wideband Radome Design. *IEE Colloquium On Advances In Electromagnetic Screens*, pp. 7/1-7/6.

55. M. R. Chaharmir, J. Shaker, and H. Legay. (2008). FSS-backed reflectarray with broadband square loop cell elements for dual-band application. *Antennas and Propagation Society International Symposium*, pp. 1–4.
56. M. Hajj, E. Rodes, and T. Monédière. (2009). Dual-Band EBG Sectoral Antenna Using a Single-Layer FSS for UMTS Application, *IEEE Antennas and Wireless Propagation Letters*, 8, pp. 161–164.
57. A. Munir, V. Fusco, U. Kingdom, and H. D. Technique. (2008). A Hybrid De-embedding Technique and Its Application for FSS Characterization. *Asia Pacific Microwave Conference*, pp. 1-4.
58. R. U. Nair, A. Neelam, and R. M. Jha. (2009). A novel Jerusalem cross FSS embedded A-sandwich radome for aerospace applications. *2009 Appl. Electromagn. Conf.*, pp. 1–4.
59. B. Wang, Q. Wang, A. Liao, L. Chen, and W. Mai. (2009). Design of a FSS filter with shorting stubs for compact E-plane duplexer application. *2009 3rd IEEE Int. Symp. Microwave, Antenna, Propag. EMC Technol. Wirel. Commun.*, pp. 1040–1042.
60. R. M. S. Cruz, A. G. D. Assunção, and P. H. F. Silva. (2010). A New FSS Design Proposal for UWB Applications. *International Workshop On Antenna Tehnology* , pp. 1-4.
61. G. I. Kiani and T. S. Bird. (2011). FSS Modulator for Future High Speed Communication Applications. *Asia Pacific Microwave Conference*, pp. 845–848.
62. T. Zhang, H. H. Ouslimani, Y. Letestu, a. Le Bayon, and L. R. Darvil. (2012). A low profile multilayer seventh order band-pass frequency selective surface (FSS) for millimeter-wave application. *WAMICON 2012 IEEE Wirel. Microw. Technol. Conf.*, pp. 1–4.

63. H. Y. Chen and Y. K. Chou, "An EMI shielding FSS for Ku-band applications," *Proc. 2012 IEEE Int. Symp. Antennas Propag.*, pp. 1–2, Jul. 2012.
64. G. Kiani and V. Dyadyuk. (2012). Low loss FSS polarizer for 70 GHz applications. *Proc. 2012 IEEE Int. Symp. Antennas Propag.*, pp. 1–2.
65. M. Moallem and K. Sarabandi. (2012). A Spatial Image Rejection Filter Based on Element FSS for J-band Radar Applications. *Antennas and Propagation Society International Symposium*, pp. 1-2.
66. W. Xiao-di, L. V Xu-liang, Z. Zhao-yang, and P. Bai-cai. (2012). A Design of Multi-band Stealth Compatibility with the Application of Fusion Type FSS. *International Workshop on Metamaterials*, pp. 1-4.
67. B. G. Xia, C. F. Yao, J. Huang, J. Meng, D. H. Zhang, and J. S. Zhang. (2013). Terahertz FSS for space borne passive remote sensing application. *Electron. Lett.*, 49(22), pp. 1398–1399.
68. H. Liu, K. L. Ford, and R. J. Langley. (2008). Miniaturised bandpass frequency selective surface with lumped components. *IEEE Electronics Letters*, 44(18), pp. 1054-1055.
69. M. Yang, A. K. Brown, and S. Member. (2010). A Hybrid Model for Radio Wave Propagation Through Frequency Selective Structures (FSS)," *IEEE Trans. Antennas Propag.*, 58(9), pp. 2961–2968.
70. M. Ying, T. Hori, M. Funmoto, T. Se, K. Sato, and I. Oshima. (2013). Unit Cell Structure of AMC with Multi-Layer Patch Type FSS for Miniaturization. *IEEE Trans. Antennas Propag.*, 2, pp. 957–960.
71. X. Meng and A. Chen. (2009). Influence of cross-loop slots FSS structure parameters on frequency response. *2009 3rd IEEE Int. Symp. Microwave, Antenna, Propag. EMC Technol. Wirel. Commun.*, pp. 939–942.

72. A. Edalati, S. Member, T. A. Denidni, and S. Member. (2011). High-Gain Reconfigurable Sectoral Antenna Using an Active Cylindrical FSS Structure. *IEEE Trans. Antennas Propag.*, 59(7), pp. 2464–2472.
73. A. Qing and C. K. Lee. (2001). An Improved Model for Full Wave Analysis of Multilayered Frequency Selective Surface with Gridded Square Element. *Prog. Electromagn. Res.*, 30, pp. 285–303.
74. S. K. Tripathy, B. P. Hota, and P. V Rajeswari. (2013). Study of Optical Characteristics of Tin oxide thin film prepared by Sol-Gel Method. *Bull. Master Sci.*, 36(7), pp. 1231-1237.
75. Z. Jin, H.-J. Zhou, Z.-L. Jin, R. F. Savinell, and C.-C. Liu. (1998). Application of nano-crystalline porous tin oxide thin film for CO sensing. *Sensors Actuators B Chem.*, 52(1-2), pp. 188–194.
76. V. Baranauskas, M. Fontana, Z. J. Guo, H. J. Ceragioli, and A. C. Peterlevitz. (2005). Field-emission properties of nanocrystalline tin oxide films. *Sensors Actuators B Chem.*, 107(1), pp. 474–478.
77. H. N. Lee, B. J. Song, and J. C. Park. (2014). Fabrication of p-Channel Amorphous Tin Oxide Thin-Film Transistors Using a Thermal Evaporation Process. *J. Disp. Technol.*, 10(4), pp. 288–292.
78. C. Lin, D. Zhang, and X. Liu. (2012). A study of tin oxide thin film gas sensors with high oxygen vacancies. *2012 7th IEEE Int. Conf. Nano/Micro Eng. Mol. Syst.*, pp. 693–697.
79. P. J. Kelly and R. D. Arnell. (2000). Magnetron sputtering : a review of recent developments and applications,” 56, pp. 159–172.
80. S. Baco, A. Chik, and F. Yassin. (2012). Study on Optical Properties of Tin Oxide Thin Film at Different Annealing Temperature. *Journal of Science and Technology*, 4(1), pp. 61-72.

81. G. Xiaoyong, F. Hong-Liang, Z. Zeng-Yuan, M. Jiao-Min, Z. Meng-Ke, C. Chao, G. Jin-Hua, Y. Shi-E, C. Yong-Sheng, and L. Jing-Xiao. (2011). Effect of the Oxygen Flux Ratio on the Structural and the Optical Properties of Silver-oxide Films Deposited by Using the Direct-current Reactive Magnetron Sputtering Method. *J. Korean Phys. Soc.*, 58(2), pp. 243.
82. N. Bin Nayan. (2008). Studies on high – pressure magnetron sputtering plasmas using laser – aided diagnostic techniques. *Nagoya University*.
83. A. S. Reddy, N. M. Figueiredo, and A. Cavaleiro. (2012). Pulsed direct current magnetron sputtered nanocrystalline tin oxide films. *Applied Surface Science*, 258(22), pp. 8902–8907.
84. G-J. Janssen. Information on the FESEM (Field-emission Scanning Electron Microscope), *Radboud Universiteit Nijmegen*, pp. 1-5. Retrieved May 14, 2014, from www.sem.com/analytic/sem.htm.
85. (1986). Non-Contact Mode AFM in Ambient Atmosphere. pp. 85–88. Retrieved May 14, 2014, from www.parkAFM.com.
86. (2004). Introduction to Grazing Incidence Diffraction. *Bruker AFS*, pp. 1–29. Retrieved May 14, 2014, from <http://mmlab.dlut.edu.cn/training/gid>.
87. S. Conference. (1998). A simple formula for calculating the frequency-dependent resistance of a round wire. *Microwave and Optical Technology Letters*, 19(2), pp. 84–85.
88. G. I. Kiani, A. Karlsson, and L. Olsson. (2007). Glass Characterization for Designing Frequency Selective Surfaces to Improve Transmission through Energy Saving Glass Windows. *Asia Pacific Microwave Conference*, pp. 1-4.
89. M. Kolif. (2001). Relationships among Properties of Sputtered Thin Films and Sputtering Process Parameters. *International Spring Seminar On Electronic Packaging*, pp. 42–46.

90. G. Korotcenkov, V. Brinzari, J. Schwank, M. Dibattista, and A. Vasiliev. (2001). Peculiarities of SnO₂ thin films deposition by spray pyrolysis for gas sensor application. *Sensors and Actuators*, 77(2001), pp. 244–252.
91. M. Keum and J. Han. (2008). Preparation of ITO Thin Film by Using DC Magnetron Sputtering. *Journal of Korean Physical Society*, 53(3), pp. 1580–1583.



PTTA UTHM
PERPUSTAKAAN TUNKU TUN AMINAH